


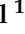



Article

Unwanted Supplementary Vibrations of Helicopter Radio Communication Systems

Marek Češkovič¹, Martin Schrötter¹, Róbert Huňady², Pavol Kurdel¹ and Natália Gecejová^{1,*}¹ Faculty of Aeronautics, Technical University of Košice, Rampová 7, 041 21 Košice, Slovakia² Faculty of Mechanical Engineering, Technical University of Košice, Letná 1/9, 042 00 Košice, Slovakia

* Correspondence: natalia.gecejova@tuke.sk; Tel.: +421-55-602-6149

Abstract: A helicopter in flight can be considered an unstable dynamic system with many unwanted vibrations originating from multiple sources, such as the operation of the engines and individual components. These vibrations cause the degradation of the structural and functional components of a helicopter, thereby generally reducing the utility and technical efficiency of the aircraft. During the analysis of frequently recurring errors of medium-heavy helicopters, partial damage to antenna elements with vertical polarisation was detected. These damages provided the basis for the presented research, based on which supplementary vibrations caused by unwanted electromagnetic oscillations were revealed. These oscillations were detected in the process of communication between the helicopter crew and the ground ATC (air traffic control) station. This phenomenon's existence and negative influence were confirmed via measurements and modal analysis, based on which an exact synergy between harmonic frequencies of the helicopter's normal vibrations was discovered. The obtained results serve as a theoretical and practical basis for the future monitoring of this phenomenon, especially in the process of determining the "health status" of medium-heavy helicopters.

Keywords: antenna; communication system; helicopter; modal analysis; vibration



Citation: Češkovič, M.; Schrötter, M.; Huňady, R.; Kurdel, P.; Gecejová, N. Unwanted Supplementary Vibrations of Helicopter Radio Communication Systems. *Aerospace* **2023**, *10*, 632.

<https://doi.org/10.3390/aerospace10070632>

Received: 22 June 2023

Revised: 7 July 2023

Accepted: 11 July 2023

Published: 13 July 2023



Copyright: © 2023 by the authors. Licensee MDPI, Basel, Switzerland. This article is an open access article distributed under the terms and conditions of the Creative Commons Attribution (CC BY) license (<https://creativecommons.org/licenses/by/4.0/>).

1. Introduction

Any movement, i.e., a manifestation of force, desirable or undesirable, has a significant effect on the structural elements of a helicopter, including the antenna elements [1]. It is, therefore, necessary to examine the given area and describe it in detail, as the problem of corrective instability of helicopter flight is caused by the influence of the forces accompanying the flight [2–4]. These forces can have both a positive and a negative effect, and the helicopter is affected by them—ideally within the limits set for operational safety and the purpose of use [5]. This characteristic of moments of forces is formed by the sums of negative forces—vibrations, which contribute to the balanced flight of the helicopter [6]. Vibrations caused by helicopter design and technology, including radio-communication antennas during transmission, have the characteristic of a random process [7,8]. This process can be described by time functions containing one or more random, time-independent parameters, which are characteristic of helicopter power systems, producing the highest number of vibrations [7,8].

The individual phases of helicopter flight are accompanied by typical, expected and well-described mechanical vibrations [6–8]. The source of higher harmonics in the area of a helicopter's vibration band is from the take-off mode to the stabilisation of the flight and then the braked landing mode of the helicopter. In addition, constant harmonic vibrations can be recorded in the hover mode [8]. Local areas (elements of the system of the helicopter) producing mechanical vibrations affecting the structural surface and equipment of the helicopter can be described in the following figure (Figure 1), representing the vibration environment of the helicopter. This environment combines many vibrating elements—main rotor, tail rotor, reducer, and motor. Since vibrations are transmitted to the surrounding

environment and subsequently to the helicopter's fuselage, acoustic vibration measurement is a suitable indicator for measuring mechanical vibrations.

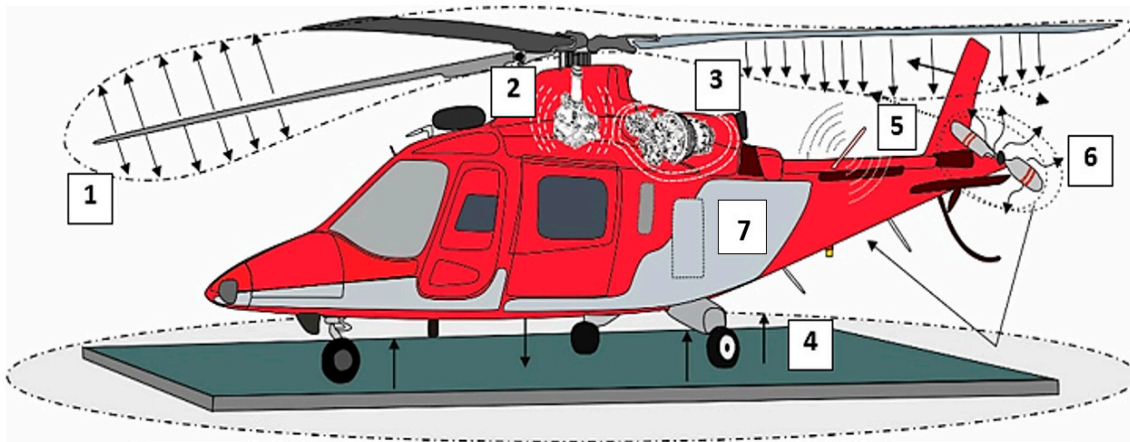


Figure 1. The local areas (elements of the system of the helicopter) producing mechanical vibrations affect the helicopter's structural surface and components. **Legend:** 1. vibration of the carrier rotor blades; 2. vibration from the reducer; 3. vibration from engines; 4. vibrations from the Earth's surface; 5. investigated supplemental vibration of the antenna element during transmission; 6. vibration from the balancing rotor; 7. vibrations from the structure of the helicopter fuselage.

Individual mechanical vibrations produced by helicopter systems can be described as components of harmonic oscillations with random initial phases. A set of oscillations in which the amplitudes are determined can be determined for each helicopter component, assuming that the phase of the oscillating signal is distributed evenly over the transients associated with the helicopter's vibrations [6–8]. This phenomenon can be described using the vibrational correlation function (1) [9,10]:

$$K(\tau) = \frac{A_0^2}{2} \cos \bar{\omega}_0 \tau \quad (1)$$

where

$K(\tau)$ is the vibrational correlation function;
 A_0 is the initial amplitude of the vibration;
 $\bar{\omega}_0$ is the initial angular frequency of the vibration;
 τ is the variable time difference ($\tau = t_2 - t_1$). The spectral density at frequency $\bar{\omega}$ is expressed by Equation (2):

$$G(\bar{\omega}) = \pi A_0^2 \delta(\bar{\omega} - \bar{\omega}_0) \quad (2)$$

where

G is the spectral density;
 π is the Ludolphine number;
 A_0 is the initial amplitude of the vibration;
 δ is the function for determining the start of the vibration;
 $\bar{\omega}$ is the angular frequency of the vibrations;
 $\bar{\omega}_0$ is the initial angular frequency of the vibration.

The helicopter represents a moving resonating element that creates a finite broadband vibration, containing many harmonic components. The overall process can be described as a summation of multiple random parameters from multiple helicopter systems (Equation (3)) [9,10].

$$x_{\Sigma}(t) = \sum_{i=1}^n A_{0i} \sin[\bar{\omega}_{0i} t + \phi_i(t)] \quad (3)$$

where

$x_{\Sigma}(t)$ is the sum of the harmonic components from the elements of the system of the helicopter, causing the vibration;

A_0 is the initial amplitude of the vibration;

$\bar{\omega}_0 i$ is the initial angular frequency of the vibration from the i -th system of the helicopter, causing the vibration;

t is the time;

$\phi_i(t)$ is the phase change upon reflection.

The very manifestation of the components and their vibrations differ in frequencies or amplitudes. In the second case, the one-dimensional probability density takes the form of Equation (4):

$$P(x) = \int_x^{\infty} \frac{p(A)}{\pi \sqrt{A^2 - x_{\Sigma}^2}} dA \quad (4)$$

where

$P(x)$ is the probability density of the vibrations;

$p(A)$ is the distribution law of the amplitudes;

π is the Ludolphine number;

A is the amplitude of the vibration;

x is the harmonic components of the vibration.

Overall, the individual components of the vibrations produced by the helicopter systems create the result of the overall vibration. These are narrow-band vibrations that are classified in the group of quasi-harmonic oscillations. Quasi-harmonic vibrations are produced when a random broadband vibration (for example, from helicopter engines) is applied to an oscillating system formed by a helicopter structure as a model of a single-degree-of-freedom system with damping. This is subsequently partially transferred to the helicopter's antenna elements, which are loaded by mechanical manifestations of vibrations from the helicopter's structural elements [11–16].

Antennas, one of the most critical devices on aircrafts and helicopters for communication and radio-technic equipment, are devices used to transform high-frequency current into electromagnetic (radio) waves when transmitting and transforming radio waves into high-frequency current when receiving [17–19]. From the physical point of view, the antenna is a conductor with a designated length that depends on its desired parameters, such as operating (resonant) frequency and radiation pattern. Other parameters, such as physical dimensions and internal construction, rely on the intended purpose (communication; navigation) [20–24].

Modern antennas must be complex to achieve the best performance of wireless communication links. They must withstand not only different environmental conditions but also their quick changes, especially in temperature and g-force. As a compromise between their physical dimensions, electrical properties, and performances, manufacturers use some standard solutions—tuning the antenna's circuit into a resonant state when the capacitive and inductive reactances cancel each other out. Thus, the antenna must be equipped with a coil [25–28].

For best performance, the antenna must be tuned to its resonant frequency, and at the same time, it must be matched to the circuit in terms of electrical properties. As the antenna represents a resonant circuit, the electric coils are used for fine-tuning its impedance. These coils can also increase inductance and thus provide ideal coupling to the transceiver. Coils are usually self-supporting or wound around the Teflon support structure. However, the significant increase in weight when the coil is used affects the antenna vibration and g-force, so antenna designers must consider it [27,28].

When the antenna is connected to the transmitter, and high-frequency current flows through its turns, this current produces a force between these turns, which can be expressed as Equation (5):

$$F_f = \frac{\mu I l}{2\pi a} \quad (5)$$

where

F_f is the force between turns of coil;
 μ is the permeability of the material;
 π is the Ludolphine number;
 a is the distance between coil turns;
 I is the electric current;
 l is the length of the coil turn.

The currents flowing to the antenna and its turns are of a high amplitude (several Amperes) during transmission. Such currents will create a significant force between the coil turns. As these currents alter in time, so the force will be changed, resulting in the movement of coil windings [29].

A more detailed analysis of the mechanical vibration measurements of the helicopter, which showed abnormalities when examining the radio communication antenna elements, prompted the authors' team to establish a research hypothesis.

Hypothesis: is it possible that the relatively frequent breakage of helicopter antenna elements is caused not only by mechanical vibrations but also by vibrations associated with radio communication transmission and, thus, by electromechanical vibrations?

2. Materials and Methods

Vibrations should be understood as unwanted, persistent oscillations (oscillations), mainly of a mechanical nature, originating from the already mentioned components of the helicopter and transmitted to the entire helicopter system.

The forces and moments acting from the vibration-producing components (Figure 1) are added following the theory of the cumulative result (Equation (6)) [9,10] as follows:

$$x_{\Sigma}(t) = \sum_{i=1}^7 X_1 + X_2 + \dots + X_7 \quad (6)$$

where

$x_{\Sigma}(t)$ is the sum of the harmonic components from the elements of the system of the helicopter, causing the vibration;

X_i is the element of the i -th system of the helicopter, causing the vibration.

The overall applied forces, F , are transferred to the helicopter's fuselage and cause it to oscillate. Such vibrations are typical of all helicopters because they are created by the forces and moments that arise during the normal operation of the moving parts of the helicopter, especially its rotating parts. These vibrations are called normally conditioned vibrations. The resulting applied force, parallel to the axis of the helicopter fuselage, causes the fuselage to bend in its vertical plane. The force rotating in the plane of rotation of the helicopter blades causes bending vibrations of the fuselage in the vertical plane and bending-torsional, i.e., transverse vibrations, in which the helicopter fuselage bends in the horizontal plane and twists around its longitudinal axis. These forces act on the antenna's moment attachment and other helicopter systems attached to the fuselage [2–5,13–16].

Per the rules of addition, the forces acting on the fuselage contain only harmonics, which are a multiple of the total number of frequencies acting on the helicopter as vibrations. Of practical significance is usually only the circular frequency of the helicopter fuselage oscillations, which is affected by the number of propellers of the carrier rotor and the ratio of the frequency of the excitation force to the inherent frequencies of the helicopter fuselage. As the number of rotor blades increases, the number of transient harmonics increases in accordance with the addition rules. In general, their value decreases as the number of rotor blades increases [14,15].

Based on the mechanical, vibration-induced movements of the helicopter structure, a relationship is established between the oscillations and the ideal position of the antenna elements of the systems. This position must be designed in order to maintain the highest possible parameters of the antenna elements, to which the gain and radiated power of

the antenna are adjusted without the effect of the attenuation of the helicopter fuselage. The idea is to create an anti-vibration system that will prevent this negative effect on the antenna elements.

In the construction of a helicopter as a vibrating device, another of the many problems is the surface tension dispersing along the fuselage of the helicopter, which is often proportional to the vibration amplitudes. Amplitudes of vibrational displacements can be used to estimate stresses in the structural materials of antenna systems, considering their stiffness [2,3,14,15].

In the general case, these vibrations can be expressed in a Fourier series as a sum of harmonic oscillations with frequencies that are multiples of the fundamental found frequency, which depends on the parameters of the helicopter—the number of rotor blades, and the number of the helicopter engines (Equation (7)) [9,10].

$$S = \sum_{i=1}^{\infty} S_{ai} \cos(\bar{\omega}t + \beta_i) \quad (7)$$

where

S is the vibrational shift;

S_{ai} is the amplitude of the vibrational shift from the i -th system of the helicopter, causing the vibration;

β_i is the phase shift angle of the i -th harmonic component;

$\bar{\omega}$ is the angular frequency of the vibrations;

t is the time.

Creating a realistic idea of poly-harmonic oscillations is necessary to know the vibration displacement amplitude, angular frequency and phase displacement angle for each of the vibration components from the systems producing the vibrations on the helicopter. Many difficulties and design failures can be avoided by identifying and quantifying the two main parameters—the amplitude and frequency of vibration displacement on the helicopter. It goes without saying that only mechanically and structurally approved and undamaged components (in our case, tested antenna elements), correctly and appropriately placed on the surface of the helicopter, are taken into account during the analysis [2,3,14,15].

However, during the operation of the helicopter, due to manufacturing and installation errors (for example, the weight imbalance of the rotor blades, aerodynamic difference of the rotor blades, and uneven rotation of the rotors), the discrete lines of the spectrum of polyharmonic oscillations are detuned. As a result, the real spectrum is not linear but quasi-poly-harmonic, which is described by the following Equation (8):

$$S(t) = \sum_{i=1}^n S_{ai}(t) \cos(i\omega_1 t + \beta_i(t)) + S_{\zeta}(t) \quad (8)$$

where

$i\omega_1$ is the average frequency of the narrowband vibration process of the systems of the helicopter, causing the vibration;

S_{ai} is the amplitude of the vibrational shift from the i -th system of the helicopter, causing the vibration;

$\beta_i(t)$ is the random and slowly varying phase shift angle of the i -th harmonic component;

$S_{\zeta}(t)$ is the noise component of the vibration signal originating from the systems of the helicopter, causing the vibration.

In the case of the presented research and the solved hypothesis, the attention is focused primarily on difficulties and structural failures, and the breakage of the antenna elements of the radio communication systems of the helicopter (Figure 2), caused by vibrations.

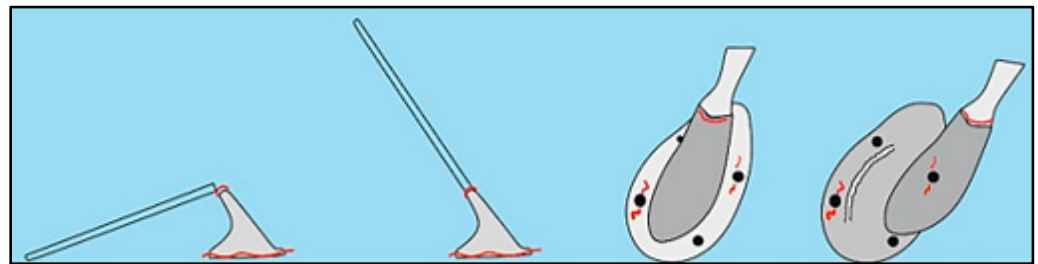


Figure 2. Visualisation of the statistically most frequently occurring damages to and breakages of a helicopter's radio communication antenna.

As shown during the acoustic measurements of mechanical vibrations, and as will be described in detail, during the transmission of radio communication antennas, additional vibrations are created caused by the very transmission of the voice radio communication message through the antenna. This supplementary vibration has the same negative impact on the construction of the antenna system as the already-known mechanical vibrations do [18].

One reason for breaking the radio communication system's antenna element is the addition of other onboard systems with close frequencies, which creates oscillations in the form of nomenclature beats. As will be analysed in the article, these blows can cause an impact force factor, which breaks the disturbed or otherwise damaged component (in the presented case, the antenna element) at the weakest point, as shown in the figures (Figures 2 and 3).

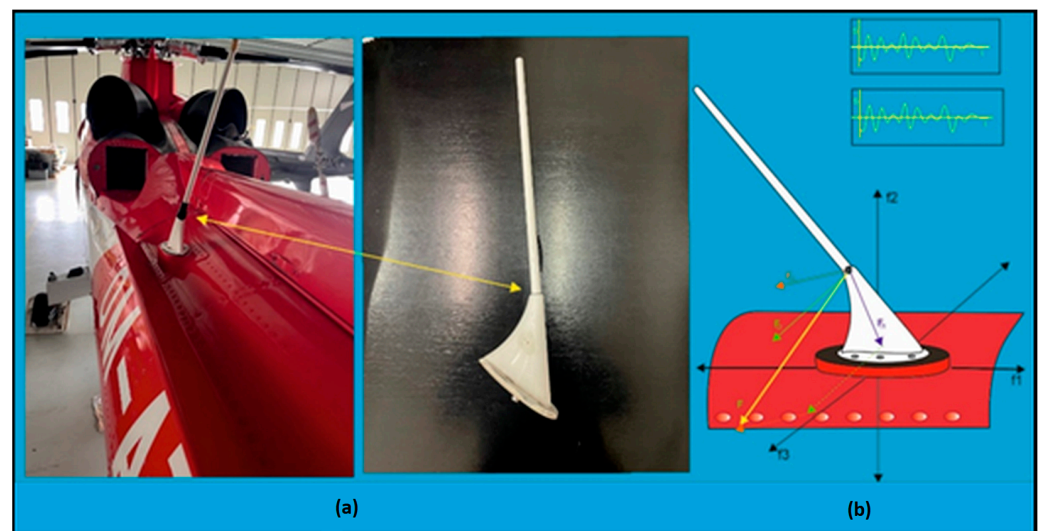


Figure 3. Photo documentation of the gradual deformation of the radio communication antenna. (a) Radio-communication antenna type CI 200 attached to the structure of the helicopter by a riveted connection; (b) radio communication antenna type CI 200—visualisation of acting forces and vibration frequencies during the action phase of the helicopter's straight-line flight.

In the nomenclature hit, the frequency of oscillations is deviated from the average value, and oscillations can be expressed as random variables changing almost periodically, with a constant frequency, random amplitude and random phase. While the amplitudes are functions of time, slowly changing in time compared to the force loading of the element, which is expressed by Equation (9):

$$F = F_a(t)\cos[\bar{\omega}t + \beta(t)] \quad (9)$$

where

F is the force load of the investigated element;
 $\bar{\omega}$ is the angular frequency of the vibrations;
 $F_a(t)$ is the randomly varying amplitude of the force load of the investigated element;
 $\beta(t)$ is the randomly varying phase shift angle;
 t is the time.

The load distribution, F , is assumed according to the normal law, with the phase ranging from 0 to 2π . For these functions, the load amplitude density corresponds to the Rayleigh distribution. The distribution function of Rayleigh's law can be obtained by integrating its probability density (Equation (10)) [30,31] as follows:

$$F = \sigma \sqrt{-2 \ln(1-x)}; 0 \leq x < 1 \quad (10)$$

where

F is the force load of the investigated element;
 σ is the standard deviation from the force load of the investigated element.

The Rayleigh probability density itself is satisfactorily confirmed by the evaluation of the obtained experimental data from vibration sources (Figure 1; points 1–7), in which the supplementary vibration solved based on the established hypothesis is included; see Equation (11) [30,31]:

$$2F_{akmax} < \sum_{i=1}^N F_{ai} \quad (11)$$

where

F_{akmax} is the most significant force load from the vibration amplitudes acting on the antenna, which mainly contributes to substantial problems in the occurrence of mechanical issues with communication antennas installed on the helicopter;

F_{ai} is the amplitude of the force load of the investigated element of the i -th system of the helicopter, causing the vibration;

N is the number of helicopter systems causing the observed vibrations.

This Rayleigh distribution for non-negative-valued random variables also corresponds to the experimentally measured data obtained during the routine vibration control of the Agusta K109 helicopter (Figure 4).

The mentioned estimate of possible vibrations is carried out by monitoring the mechanical vibrations of the helicopter according to prescribed routine work and procedures. Thanks to the mandatory monitoring of mechanical vibrations, anomalies were observed in the case of helicopter antenna elements, which, in addition to the influence of mechanical vibrations transmitted from the structural components of the helicopter, also showed a supplementary vibration component—manifested only in the radio communication broadcast (Figure 4e)). The emergence of electromechanical vibrations of antenna elements is associated with high-frequency transmission (high amplitude values, and high transmission power), during which changes were observed in the winding of the antenna coil.

The focus of the presented research is primarily directed to the damage or breakage of the components of the radio communication system, the antenna, as a result of mechanical vibrations transmitted from the helicopter, but also supplementary vibrations, which were observed and captured by the author's team during the measurement of vibrations on the Agusta A109K2 helicopter. This is despite the fact that most of the helicopter's systems were shut down. The exception was the radio communication equipment designed to communicate with the helicopter pilot via the built-in radio station. In this original measurement of mechanical vibrations, despite the inactivity of the helicopter's mechanical systems, vibrations were measured at the level of the acoustic band—during voice communication with the pilot.

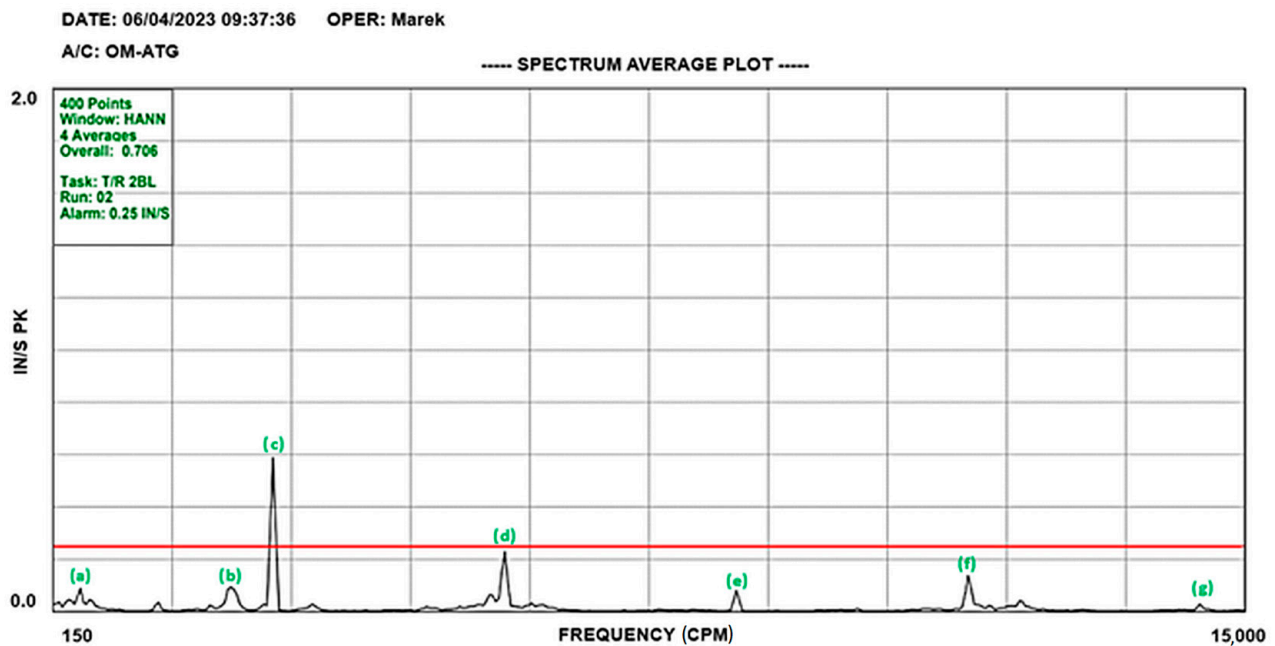


Figure 4. Results of the vibration measurements in the real conditions and graphical representation of seven vibration sources' effect on the Augusta A109K2 helicopter. **Legend:** (a) the vibration of the carrier rotor blades; (b) the vibration from the balancing rotor; (c) the vibration from the reducer; (d) the vibration from engines; (e) the investigated supplemental vibration of the antenna element during transmission; (f) the vibrations from the structure of the helicopter fuselage; (g) the vibrations from the Earth's surface.

Subsequently, verification and test measurements were carried out in a specialised laboratory, aiming to exclude an accidentally captured signal, a vibration, caused by the mechanical transmission of the voice through the helicopter's fuselage [29]. Extension measurements were started based on the positive results and, therefore, the exclusion of the capture of mechanical vibration from the fuselage of the helicopter. During these measurements, an experimental modal analysis of the base plane of the antenna during its transmission was performed.

The reason for focusing on this new phenomenon was mainly due to the negative effect of vibrations arising and transmitted through the helicopter on the radiating/receiving antenna elements and their negative influence on the gain, efficiency, impedance, voltage standing wave ratio, bandwidth or antenna polarisation.

The aforementioned mechanical vibrations from the blades of the main rotor, reducer, motors, levelling rotor, ground surface or helicopter surface negatively affect the antenna's radiation characteristics. For this reason, considerable attention has already been paid to this issue in research focused on ground applications [18,19] and on applications in aviation [20–22].

In other studies [32–34], authors dealt with the modal analysis of antennas, which have exact characteristics for different modes in terms of electric current distribution. Modal analysis of antennas is mainly used to analyse ultra-bandwidth antennas using narrowband slots embedded in planar geometry. Given the focus of this article, it should be clarified that these publications do not include classical, i.e., experimental modal analysis that investigates modal parameters based on mechanical excitation. Those with the upcoming vibration of the helicopter complete the problem of parameter changes as well as damage to the antenna itself. Other publications [35–38] are devoted to the experimental modal analysis of the structures of the helicopter on which the antennas are fixed.

From the mentioned references, but also from further research, it follows that the authors focused on the effect of external vibrations (vibrations of the helicopter's structural surface or the antenna mounting itself) on its radiating/receiving properties, or the influ-

ence of vibrations on the mechanical properties of the antenna mounting and the vibrations of the experimental base plate of the antenna as a basis for obtaining exact values and characteristics of the antenna and changes in radiation.

For this reason, the presented research focuses on a hitherto unexplored phenomenon—the electromagnetic vibration of the antenna arising during the transmission of a voice message, which can lead to damage to and the breakage of the antenna element. As evidenced by several cases from practice in which the authors of the article, as experts in the given field, were called for consultation and expert assessment.

3. Results

To verify the authors' hypothesis, a measuring set-up with the model of the aircraft antenna was created (Figure 5).

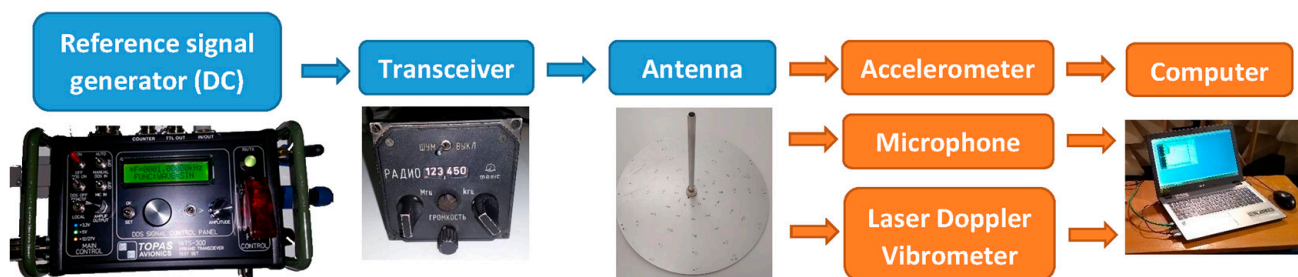


Figure 5. The block diagram of the measuring set-up.

The antenna consisted of an aluminium tube, Teflon, as a support structure for the coil, copper coil and N-type panel connector. This was mounted on an aluminium alloy sheet which served as the antenna's ground plane (ground plane). This assembly was connected to the LUN 3524 aviation transceiver for AM and the ARC 210 aviation transceiver for FM. The simple sine wave signal generator was used to achieve the constant modulating signal in the acoustic spectrum (from 200 Hz up to 3.5 kHz). This generator also had the option of setting the modulation depth, and it was connected to the transceiver, LUN 3524.

To minimise the influence of the environment (such as radio broadcasts, mobile networks, and sound noise), the whole measuring set-up was placed in the attenuation (anechoic) chamber [23].

3.1. Experimental Modal Analysis of Antenna's Ground Plane

Modal parameters were measured to assess the dynamic behaviour of the ground plane of the monopole antenna. The aim was to determine its resonant as well as anti-resonant properties for the needs of subsequent operational measurements. Due to its dimensions and shape, the ground plane can be considered a thin-walled plate whose bending stiffness is the lowest in the normal direction. For this reason, many modes can be expected to occur relatively close to each other, including overlapping modes, which guarantees an excellent dynamic response to external excitation over an extensive frequency range. In order to minimize the transmission of mechanical vibrations from the surroundings, the ground plane was suspended on four elastic cables.

The responses were measured at point ACC in the direction of its normal using a Bruel & Kjaer 4374 accelerometer. The ground plane was excited by a Bruel & Kjaer 8206 modal hammer at 60 points. This number was sufficient to render ground-plane-mode shapes of higher frequencies reliably. The position of the sensor and the method of excitation can be seen in Figure 6.

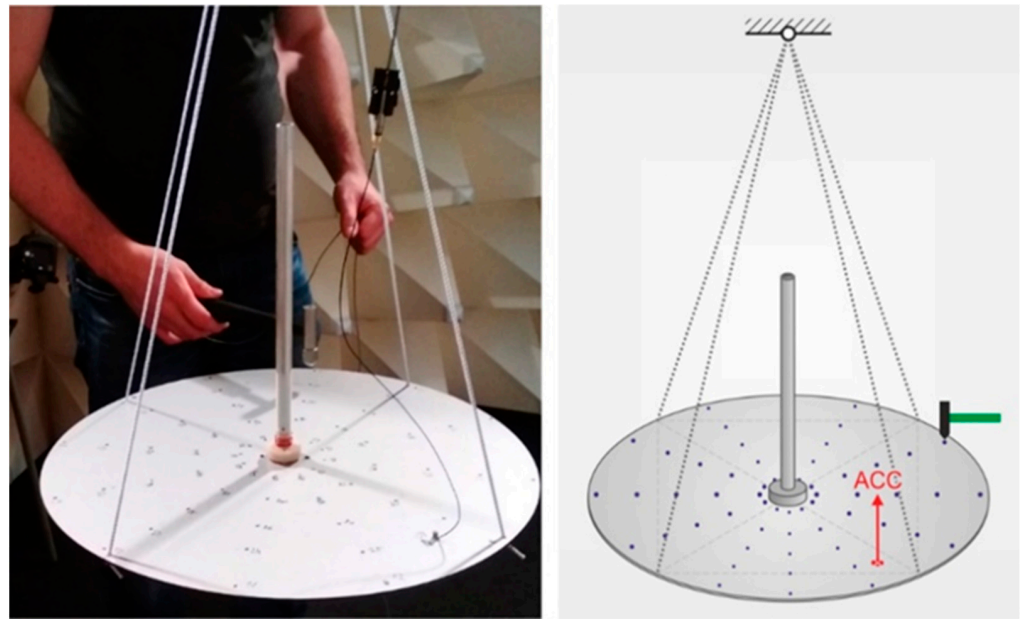


Figure 6. Experimental set-up for modal analysis of the ground plane.

The frequency range of the measurement, considering the estimated stiffness and dimensions of the ground plane, was chosen to be 5000 Hz. The measurement was evaluated in the Pulse Reflex program. A complex mode indicator function (CMIF) obtained from a matrix of measured frequency response functions (FRFs) is presented in Figure 7.

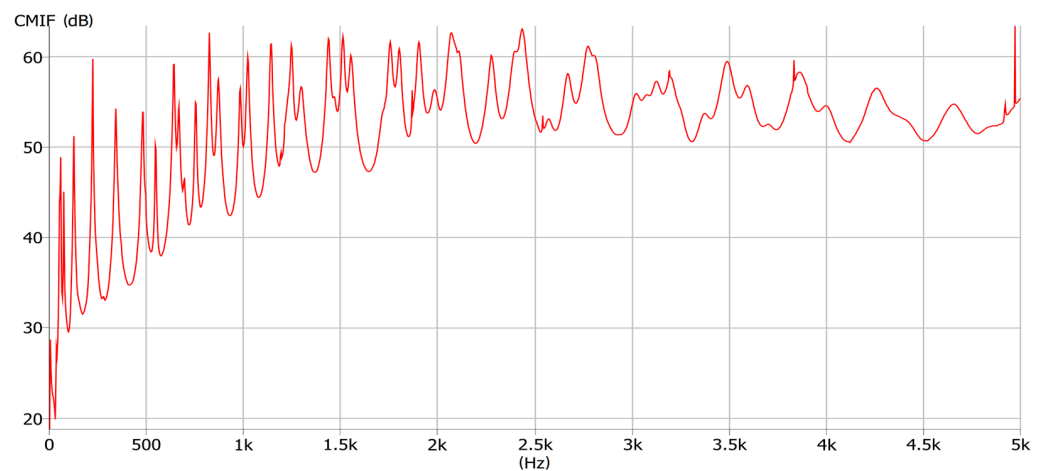


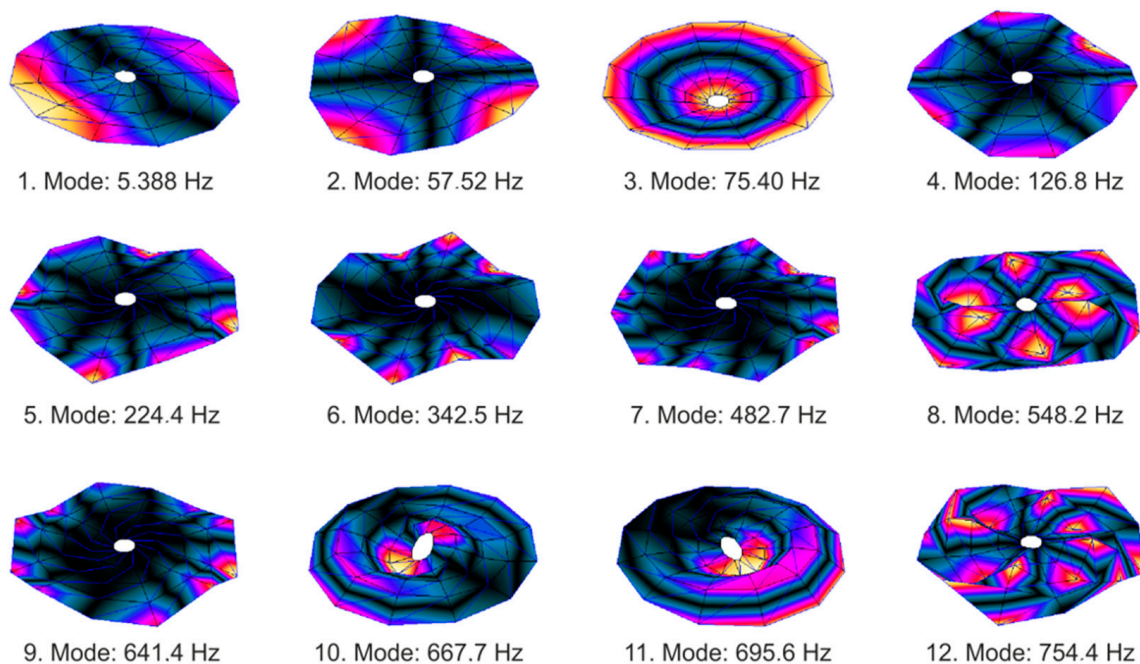
Figure 7. CMIF spectrum of the ground plane.

The Rational Fraction Polynomial-Z method was used to estimate modal parameters. The first 23 modes were evaluated in the given frequency range. Their frequencies and damping are presented in Table 1.

Higher modes, due to the nature of measurement, are not relevant. Selected mode shapes, plotted in absolute values, are shown in Figure 8. Note that due to the axial symmetry of the ground plane, the occurrence of overlapping multiple mode shapes at the same or very close natural frequencies can be assumed. However, these modes cannot be identified via SIMO (single input–multiple output) measurements.

Table 1. Natural frequencies and damping of the ground plane.

Mode	Damped Frequency (Hz)	Damping (%)	Complexity (–)
1.	5.388	16.067	0.49540
2.	57.52	0.646	0.27154
3.	75.4	0.915	0.11721
4.	126.8	1.352	0.07897
5.	224.4	0.426	0.08409
6.	342.5	0.941	0.21783
7.	482.7	0.770	0.09957
8.	548.2	0.452	0.02322
9.	641.4	0.464	0.05466
10.	667.7	0.626	0.05143
11.	695.6	0.832	0.14585
12.	754.4	0.455	0.03275
13.	824.7	0.399	0.02084
14.	871.3	0.559	0.10575
15.	983.4	0.512	0.02382
16.	1022.7	0.535	0.01933
17.	1142.1	0.493	0.01843
18.	1248.2	0.409	0.16238
19.	1297.7	1.034	0.15361
20.	1438.1	0.544	0.04233
21.	1467.0	0.609	0.14147
22.	1512.4	0.452	0.01915
23.	1554.9	0.625	0.14254

**Figure 8.** The first twelve mode shapes of the ground plane.

3.2. Vibrational Analysis of Antenna's Ground Plane during Its Radiation

The measurement aimed to determine what happens to the ground plane when the antenna transmits AM and FM signals. Two types of analyses were performed in which the antenna with a coil and the antenna without a coil were examined. The location of the antenna in the attenuation chamber and its suspension method minimised the influence of undesirable external factors.

Three different types of sensors were used to measure the vibration responses of the antenna's ground plane: the Bruel & Kjaer 4374 accelerometer (ACC), the Polytec PDV-

100 spot laser vibrometer (LDV) and the MPA416 microphone (MIC). These sensors were chosen due to their high sensitivity and large frequency range (Table 2).

Table 2. Properties of measuring sensors.

Sensors	ACC	LDV	MIC
Frequency response (Hz)	1 ÷ 26,000	0 ÷ 22,000	20 ÷ 20,000
Contact with object	yes	no	no

While the accelerometer and vibrometer measured the responses of mechanical vibration in the normal direction of the ground plane, the microphone was directed at its centre at an angle of approximately 45° and measured the acoustic response from a distance of 61 cm. The arrangement of the sensors can be seen in Figure 9.

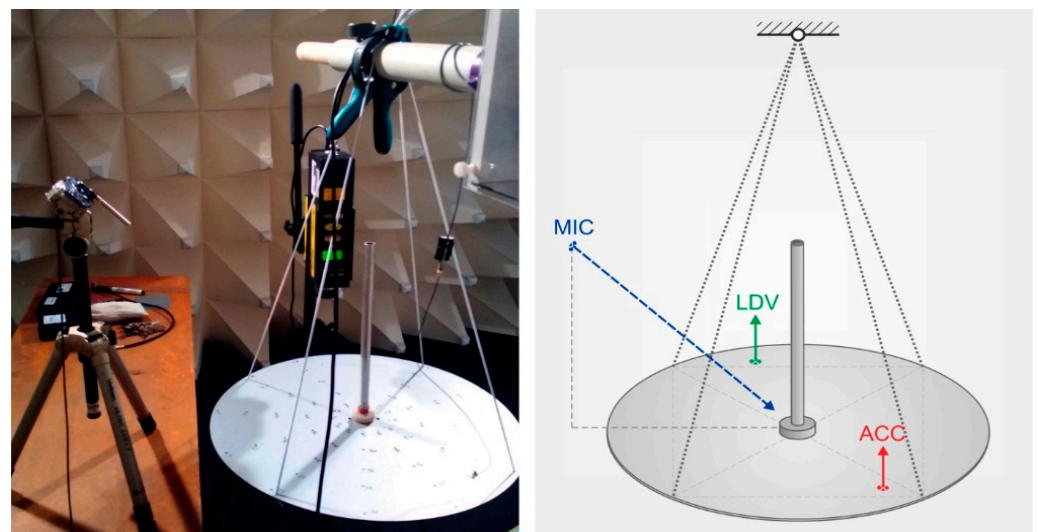


Figure 9. The experimental set-up for operating vibration analysis of the ground plane.

Several measurements were performed with different frequencies of the modulation component of the AM signal. However, the signal's carrier frequency was always the same, 122 MHz. This value was chosen deliberately, as it falls within the standard band used in aviation for radio communications (118 ÷ 137 MHz). The measurements revealed the vibrations of the ground plane, including the acoustic response, during antenna radiation.

When the antenna was transmitting the FM signal, no vibrations of the ground plane were observed in the investigated frequency spectra, so this paper did not pay further attention to it.

3.2.1. The Antenna without a Coil

The frequency spectra of the ground plane response measured during antenna transmission are shown in Figure 10, for the AM signal with a modulation frequency of 500 Hz, 1000 Hz, and 3000 Hz.

It is clear from the graphs that the ground plane was vibrating during antenna transmission without a coil. The main components of this vibration were formed by the frequency of the modulation signal and its higher harmonic frequencies. The rest of the spectrum corresponds mainly to the sensors' noise and the noise transmitted to the ground plane from the surroundings. The highest level of response was found with an accelerometer that was in direct contact with the ground plane. A slightly weaker response was recorded with a laser vibrometer. A microphone recorded the lowest level, and the sound caused by the vibrating ground plane was not audible.

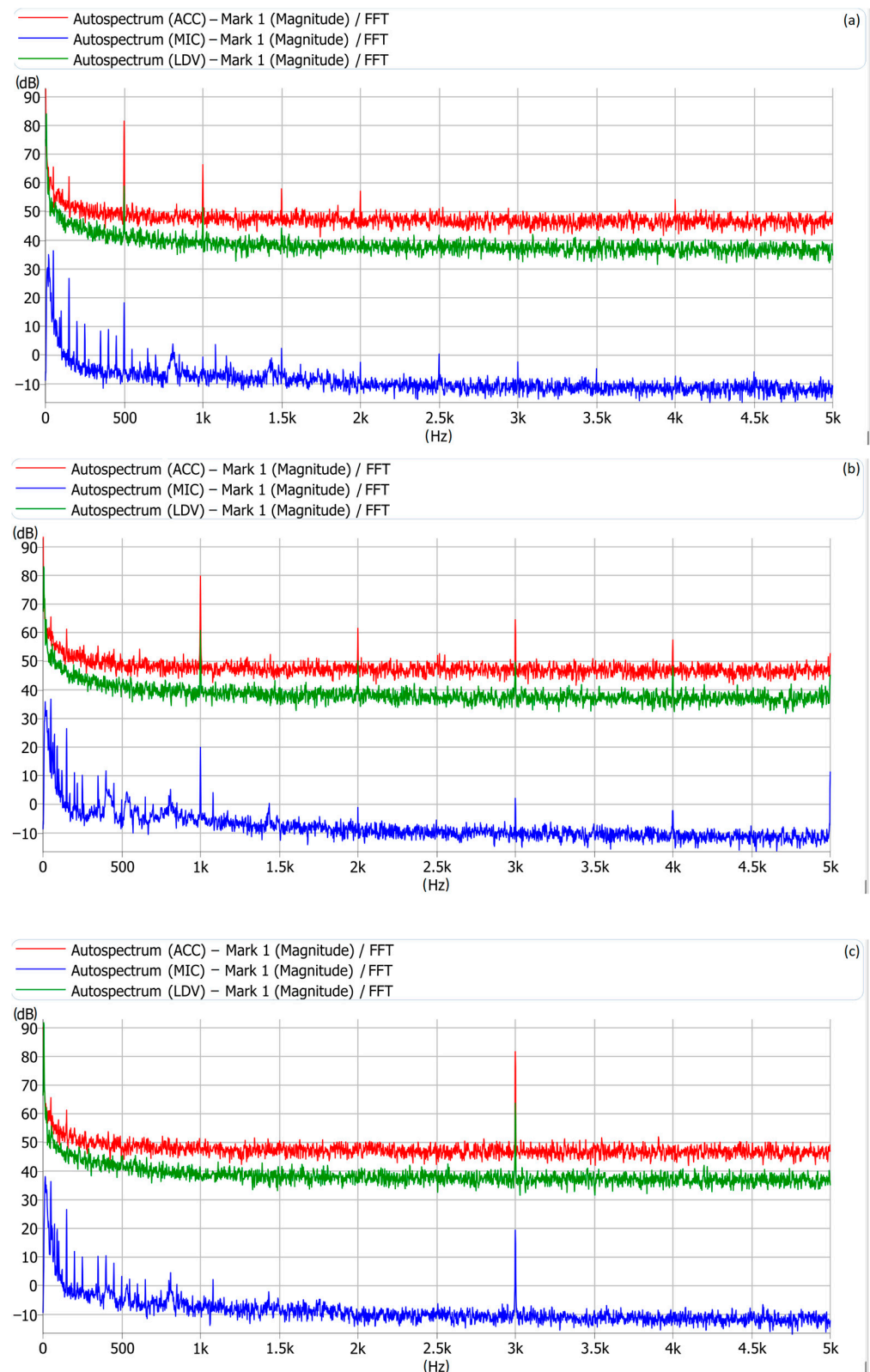


Figure 10. Response spectra of the ground plane (antenna without a coil). (a) Frequency of modulating sine wave signal: 500 Hz; (b) frequency of modulating sine wave signal: 1000 Hz; (c) frequency of modulating sine wave signal: 3000 Hz.

3.2.2. The Antenna Equipped with a Coil

The vibration measurement of the ground plane was performed under the same conditions as those described in Section 3.2.1, but here with the antenna being equipped with a coil. The response frequency spectra measured during antenna transmission are shown in Figure 11 for the AM signal with modulation frequencies of 500 Hz, 1000 Hz, and 3000 Hz.

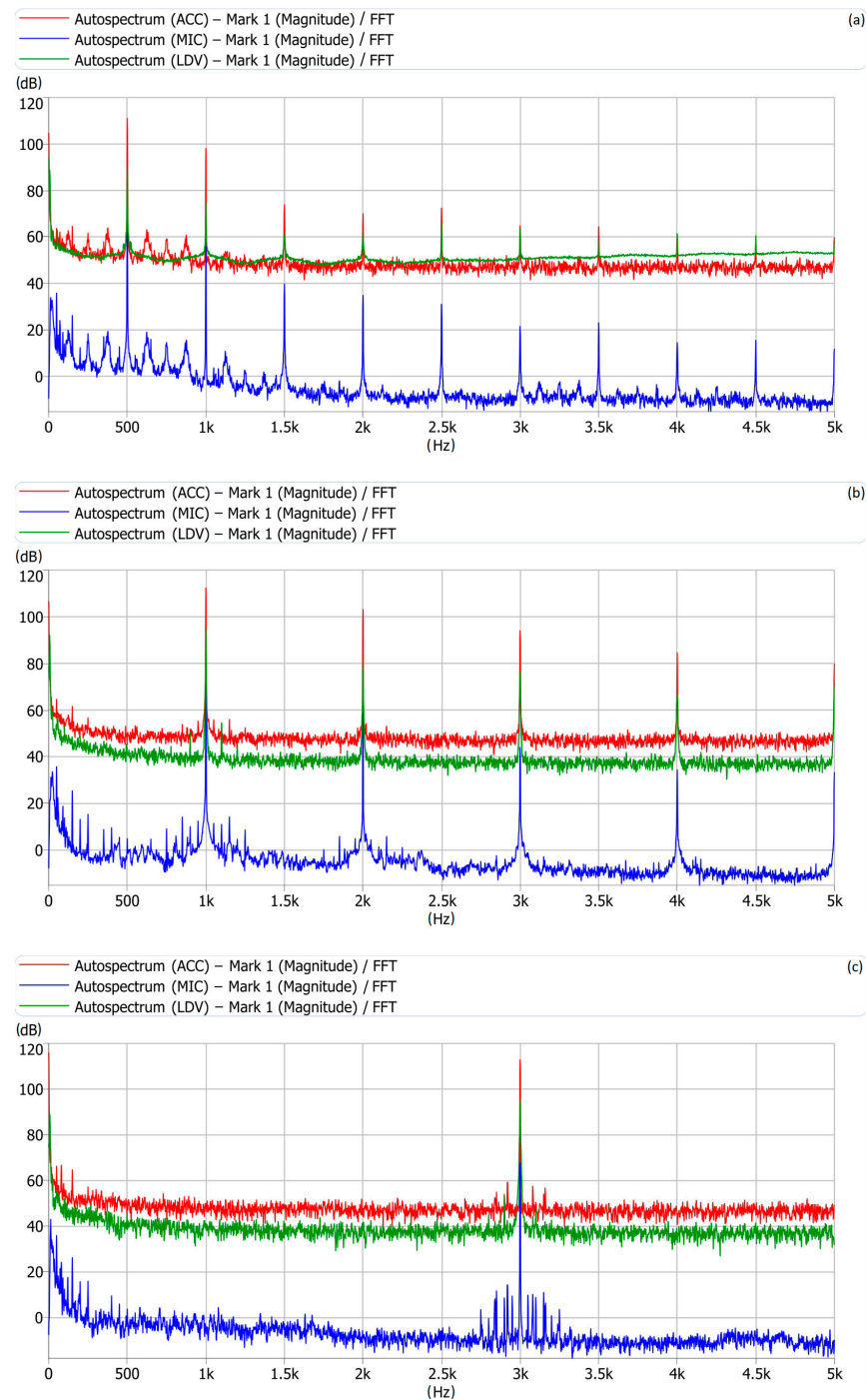


Figure 11. Response spectra of the ground plane (antenna with a coil): (a) frequency of the modulating sine wave signal: 500 Hz; (b) frequency of the modulating sine wave signal: 1000 Hz; (c) frequency of the modulating sine wave signal: 3000 Hz.

The measured response spectra prove that the ground plane vibrates during radiation in the case of an antenna equipped with a coil. The most pronounced components of this vibration again correspond to the frequency of the modulation signal and its higher harmonic frequencies. However, in this case, the amplitudes of the responses reach a much higher level. The amplification of the responses is caused by the higher radiation power of an antenna equipped with a coil compared to that of an antenna without a coil.

In the following measurement, the responses of the ground plane when excited by the modulation frequency tuned to its natural frequency of 483 Hz and when excited by the frequency of 1080 Hz falling to the off-resonant range are compared (Figures 12–14).

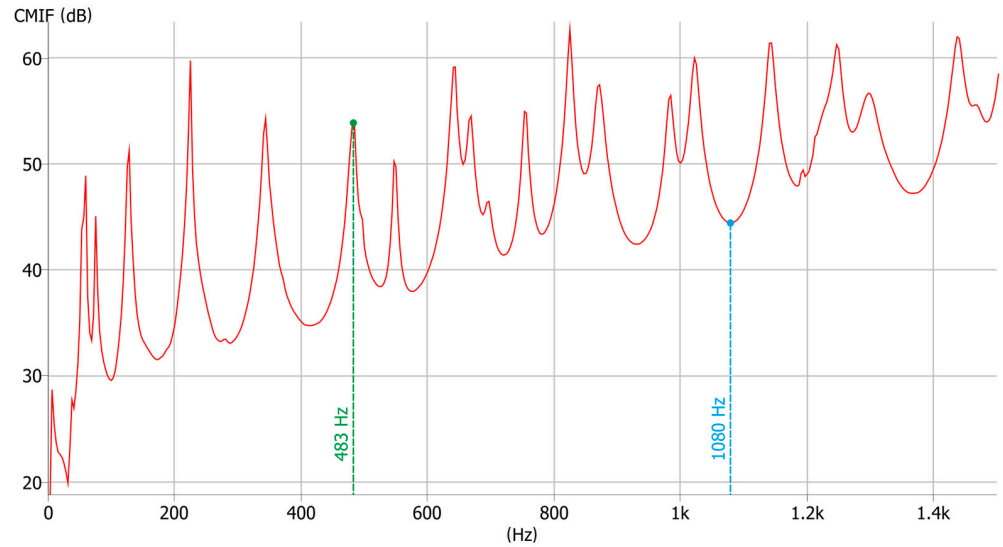


Figure 12. CMIF from frequency range 0 Hz ÷ 1500 Hz.

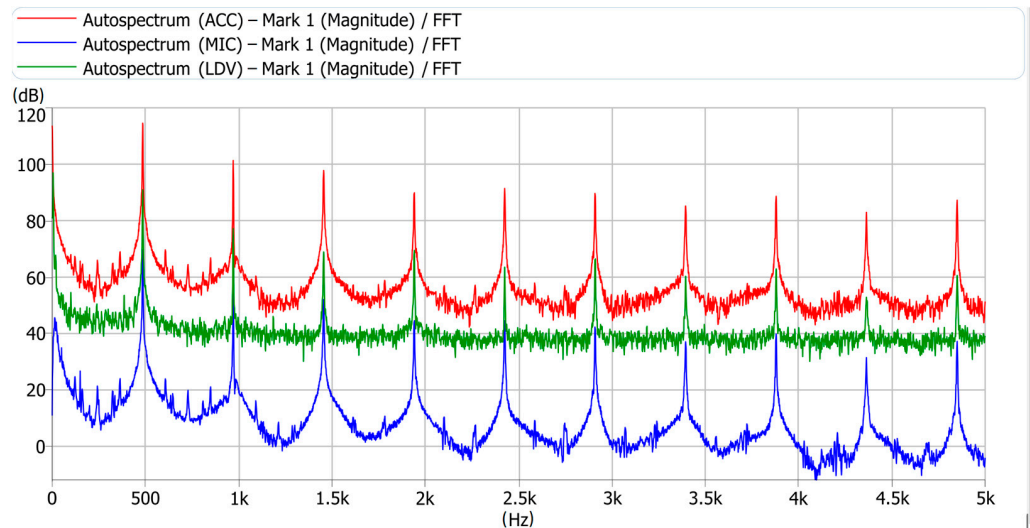


Figure 13. Response spectra of the ground plane (the antenna is with a coil). Frequency of modulating sine wave signal: 483 Hz.

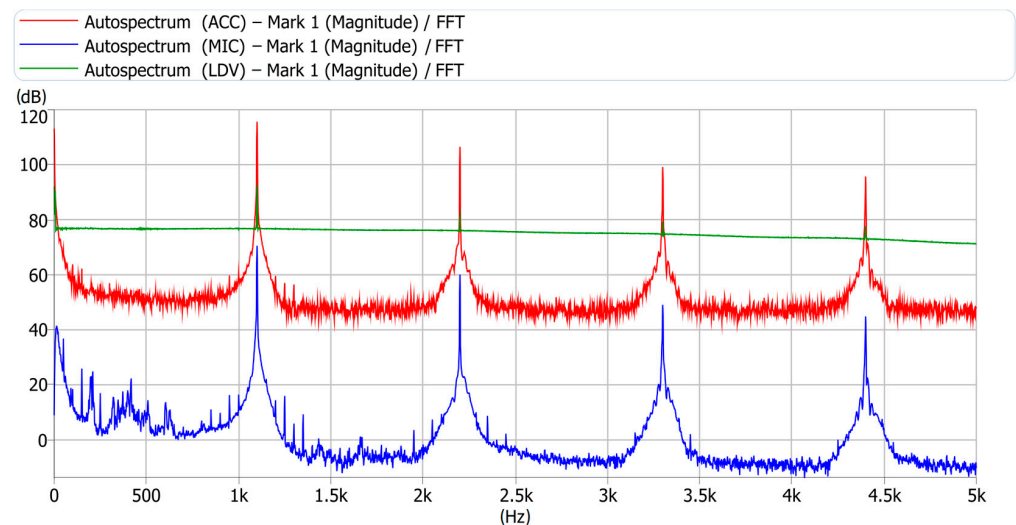


Figure 14. Response spectra of the ground plane (the antenna is with a coil). Frequency of modulating sine wave signal: 1080 Hz.

4. Conclusions

Since the measurement of the mechanical vibration responses of the ground plane was realised only at two points, it is impossible to assess the overall vibration level from the results. This can be assessed rather from the acoustic response measured using the microphone. It is also not appropriate to compare the amplitudes of the measured vibration because the shape of the ground plane vibration was different at different frequencies of the modulation signal. The root means square (RMS)/effective values of the frequency spectra of all performed measurements are presented in Tables 3 and 4.

Table 3. RMS of response spectra for different frequencies of modulating signal of antenna without a coil.

Modulation Frequency	500 Hz	1000 Hz	3000 Hz
ACC sensor	95.4 dB	106 dB	88.3 dB
LDV sensor	52.1 dB	43.6 dB	60.3 dB
MIC sensor	41.7 dB	45.9 dB	41.9 dB

Table 4. RMS of response spectra for different frequencies of modulating signal of antenna with a coil.

Modulation Frequency	500 Hz	1000 Hz	3000 Hz	483 Hz	1080 Hz
ACC sensor	112 dB	114 dB	117 dB	119 dB	119 dB
LDV sensor	60.7 dB	61.2 dB	65.8 dB	58.4 dB	63.2 dB
MIC sensor	68.1 dB	69.2 dB	67.7 dB	70.8 dB	72.0 dB

The following statements confirm the established hypothesis.

Statement 1: When the antenna is transmitting (AM), the ground plane vibrates, and the dominant components of this vibration correspond to the frequency of the modulation signal and its higher harmonic components. This is true, provided that the modulation signal is harmonic.

Statement 2: The vibration amplitudes are higher in the case of the antenna with a coil than in the case of the antenna without a coil. It follows that the vibration responses depend on the antenna's radiating power, and in general, it can be concluded that they increase with radiating power.

Statement 3: A sound effect accompanies the vibration of the ground plane.

When the antenna was transmitting the FM signal, no vibrations of the ground plane were observed in the investigated frequency band. This can be explained by the fact that the radiated power is constant during the transmission of the FM signal. This is the opposite of the AM signal, where the power changes in the rhythm of the modulating signal.

Vibration measurements of the antenna's ground plane confirmed the presence of vibration during the transmission of the AM signal. In the case of FM, no vibrations were measured.

The amplitude of measured vibrations depends on the radiated power, which is demonstrated by measurements performed on the antenna with and without the coil. The randomness of vibration presence on the ground plane was refuted by its placement in the attenuation chamber and by performing several measurements at different modulation frequencies, even at a frequency close to the anti-resonant frequency of the ground plane.

The obtained results should be used for the practical use of this phenomenon. For example, after approval, it should be one of the conditions for passing the mandatory measurements of the vibration on the helicopter and on the installed radio communication equipment, i.e., the antenna.

The next phase of our research should be the creation of a new measurement stand (also in the simulation form) for measuring not only the supplemental vibration of the antenna element during transmission but to simulate different aerodynamic loads on the antenna element, as we believe these static or dynamic loads would affect the amplitude and phase of resulting vibrations. However, the helicopter is a unique flying apparatus capable of performing different flight manoeuvres such as hovering, forward and back movement, and side movement at different speeds—the wind direction and strength must also be considered.

These movements create a G-load on the antenna and helicopter (aircraft) structure, but arising vibrations are mainly mechanical, not electromagnetic. These mechanical vibrations are measured during a regular/periodic check, provided on the ground by specialised measuring devices and maintenance staff, or rarely during flight, as an additional part of testing the mechanical vibration level.

The actual research provided by other authors is primarily focused on the mechanical vibrations of antennas (antenna arrays) or microstrip antennas caused by the movement of the object or originating from propulsors (UAV propellers) [18,39,40]. Other authors are investigating vibrations of antennas as a part of aircraft structure excited from outside electromagnetic sources but in high-frequency bands (30 MHz) [41].

Generally, we can conclude that other researchers did not investigate mechanical vibrations of the antennas during transmission caused by electronic antenna circuits operating in the Civil Aviation frequency band (118 MHz–137 MHz with amplitude modulation), so in this research article, we decided to focus on the newly found phenomenon, detected by us. For this reason, we assume our research is unique.

Our research is focused on detecting and proving the creation of supplementary electromechanical vibration during the transmission of the communication antenna. For this new type of testing, the measurement of electromechanical vibrations of the communication antennas is fully compliant, and provided measurements only on the ground during the regular/periodic check of the helicopter (aircraft).

The future of this research is in the simulation of the supplemental electromechanical vibration of the antenna element during transmission and the creation of the predicted model, which can warn maintenance staff of the interval in which it is crucial to check and consider the replacement of the communication antennas.

Author Contributions: Conceptualisation, M.Č., M.S., R.H. and N.G.; methodology, M.Č., M.S. and R.H.; software, M.Č., M.S. and R.H.; validation, M.Č., M.S., R.H., P.K. and N.G.; formal analysis, P.K. and N.G.; investigation, M.Č., M.S. and R.H.; resources, M.Č., M.S., R.H., P.K. and N.G.; data curation, M.Č., M.S., R.H. and P.K.; writing—original draft preparation, M.Č., M.S., R.H., P.K. and N.G.; writing—review and editing, M.Č., P.K. and N.G.; visualisation, R.H. and P.K.; supervision, M.S. and P.K.; project administration, M.Č., M.S., P.K. and N.G.; funding acquisition, M.Č., M.S., P.K. and N.G. All authors have read and agreed to the published version of the manuscript.

Funding: This work of M.Č., M.S., P.K. and N.G. was financed by the following project: KEGA 033TUKE-4/2023—virtual complex of aircraft and helicopter systems as a means of supporting the teaching of avionic subjects.

Data Availability Statement: Not applicable.

Acknowledgments: This work of M.Č., M.S., P.K. and N.G. was supported by the following project: KEGA 033TUKE-4/2023—virtual complex of aircraft and helicopter systems as a means of supporting the teaching of avionics subjects. The work of M.Č., M.S. and P.K. was supported by the project Mobile Monitoring System for the Protection of Isolated and Vulnerable Population Groups against Spread of Viral Diseases, ITMS code 313011AUP1, co-funded by the European Regional Development Fund under the operational programme Integrated Infrastructure. The work of author M.Č. was supported by the Slovak Research and Development Agency under contract no. APVV-20-0546.

Conflicts of Interest: The authors declare no conflict of interest.

References

- Hassan, H.S.; Bayoumy, A.M.; El-Bayoumy, G.M.; Abdelrahman, M.M. Modeling, Trimming and Simulation of a Full Scale Helicopter. In Proceedings of the 17th International Conference on Aerospace Sciences & Aviation Technology ASAT-17, Cairo, Egypt, 11–13 April 2017.
- Tommasino, D.; Moro, F.; Zumalde, E.; Kunzmann, J.; Doria, A. An Analytical–Numerical Method for Simulating the Performance of Piezoelectric Harvesters Mounted on Wing Slats. *Actuators* **2023**, *12*, 29. [\[CrossRef\]](#)
- Yang, K.; Han, D.; Shi, Q. Study on the lift and propulsive force shares to improve the flight performance of a compound helicopter. *Chin. J. Aeronaut.* **2021**, *35*, 365–375. [\[CrossRef\]](#)
- Cumbo, R.; Tamarozzi, T.; Jiranek, P.; Desmet, W.; Masarati, P. State and Force Estimation on a Rotating Helicopter Blade through a Kalman-Based Approach. *Sensors* **2020**, *20*, 4196. [\[CrossRef\]](#)
- Thiemeier, J.; Öhrle, C.; Frey, F.; Keßler, M.; Krämer, E. Aerodynamics and flight mechanics analysis of Airbus Helicopters' compound helicopter RACER in hover under crosswind conditions. *CEAS Aeronaut. J.* **2019**, *11*, 49–66. [\[CrossRef\]](#)
- Bertolino, A.C.; Gaidano, M.; Smorto, S.; Porro, P.G.; Sorli, M. Development of a High-Performance Low-Weight Hydraulic Damper for Active Vibration Control of the Main Rotor on Helicopters—Part 1: Design and Mathematical Model. *Aerospace* **2023**, *10*, 391. [\[CrossRef\]](#)
- Aggarwal, G.; Mansfield, N.; Vanheusden, F.; Faulkner, S. Human Comfort Model of Noise and Vibration for Sustainable Design of the Turboprop Aircraft Cabin. *Sustainability* **2022**, *14*, 9199. [\[CrossRef\]](#)
- Castillo-Rivera, S.; Tomas-Rodriguez, M. Hover Flight Helicopter Modelling and Vibrations Analysis. In Proceedings of the Actas de las XXXVI Jornadas de Automática, Bilbao, Spain, 2–4 September 2015.
- Liu, S.; Ling, J.; Tian, Y.; Hou, T.; Zhao, X. Random Vibration Analysis of a Coupled Aircraft/Runway Modeled System for Runway Evaluation. *Sustainability* **2022**, *14*, 2815. [\[CrossRef\]](#)
- Teng, Y.; Xie, L.; Zhang, H. Experimental Study on Vibration Fatigue Behavior of Aircraft Aluminum Alloy 7050. *Materials* **2022**, *15*, 7555. [\[CrossRef\]](#)
- Liu, S.; Tian, Y.; Liu, L.; Xiang, P.; Zhang, Z. Improvement of Boeing Bump Method Considering Aircraft Vibration Superposition Effect. *Appl. Sci.* **2021**, *11*, 2147. [\[CrossRef\]](#)
- Citarella, R.; Federico, L.; Barbarino, M. Aeroacoustic and Vibroacoustic Advancement in Aerospace and Automotive Systems. *Appl. Sci.* **2020**, *10*, 3853. [\[CrossRef\]](#)
- Kumar, J.S. Helicopter vibrations—A perspective. *Int. J. Res. Aeronaut. Mech. Eng.* **2016**, *4*, 50–63.
- Bilji, M.; Prasun, B.; Muhammad, F.; Sampit, R.; Aritra, L.; Manasa, B. A Review on Vibration Analysis of Helicopter Rotor Blade. *Int. J. Res. Appl. Sci. Eng. Technol.* **2022**, *10*, 1363–1369. [\[CrossRef\]](#)
- Mansfield, N.J.; Aggarwal, G. Whole-Body Vibration Experienced by Pilots, Passengers and Crew in Fixed-Wing Aircraft: A State-of-the-Science Review. *Vibration* **2022**, *5*, 110–120. [\[CrossRef\]](#)
- Tamer, A.; Zaroni, A.; Cocco, A.; Pierangelo, M. A numerical study of vibration-induced instrument reading capability degradation in helicopter pilots. *CEAS Aeronaut. J.* **2021**, *12*, 427–440. [\[CrossRef\]](#)
- Jiang, S.; Shuai, C.; Jiang, W.; Huang, L.; Zheng, H.; Yuan, C. Design and Experiment of Magnetic Antenna Vibration and Noise Reduction System. *Appl. Sci.* **2022**, *12*, 2450. [\[CrossRef\]](#)
- Lin, F.; Zheng, H.; Xiang, B.; Xu, R.; Jiang, W.; Lang, L. Vibration-Induced Noise in Extremely Low Frequency Magnetic Receiving Antennas. *IEEE Antennas Wirel. Propag. Lett.* **2021**, *20*, 913–917. [\[CrossRef\]](#)
- Turetken, B.; Celik, M. Analysis of vibration effects on surface matched cylindrical IFF array antenna. In Proceedings of the 2013 7th European Conference on Antennas and Propagation (EuCAP), Gothenburg, Sweden, 8–12 April 2013; pp. 2731–2735.
- Knott, P.; Loecker, C.; Algermissen, S.; Sekora, R.P. Vibration Control and Structure Integration of antennas on aircraft. In Proceedings of the 2013 7th European Conference on Antennas and Propagation (EuCAP), Gothenburg, Sweden, 8–12 April 2013; pp. 2726–2729.

21. Schippers, H.; van Tongeren, H.; Verpoorte, J.; Vos, G. Distortion of conformal antennas on aircraft structures. In Proceedings of the Smart Structures and Materials 2001: Smart Electronics and MEMS, Newport Beach, CA, USA, 5–8 March 2001; pp. 189–198.
22. Kilgore, I.M.; Kabiri, S.A.; Kane, A.W.; Steer, M.B. The Effect of Chaotic Vibrations on Antenna Characteristics. *IEEE Antennas Wirel. Propag. Lett.* **2015**, *15*, 1242–1244. [[CrossRef](#)]
23. Chung, B.; Chuah, H. Design and construction of a multipurpose wideband anechoic chamber. *IEEE Antennas Propag. Mag.* **2003**, *45*, 41–47. [[CrossRef](#)]
24. Feliu-Battle, V.; Feliu-Talegon, D.; Castillo-Berrio, C.F. Improved Object Detection Using a Robotic Sensing Antenna with Vibration Damping Control. *Sensors* **2017**, *17*, 852. [[CrossRef](#)] [[PubMed](#)]
25. Li, Z.; Yang, K.; Chen, J.; Duan, S. A Novel Fault Identification Method Using Modified Morphological Denoising via Structuring Element Optimization for Transmission Systems of Shipborne Antennas. *J. Mar. Sci. Eng.* **2022**, *10*, 190. [[CrossRef](#)]
26. Nikkhah, N.; Zakeri, B.; Abedi, H. Extremely electrically small MF/HF antenna. *IET Microw. Antennas Propag.* **2019**, *14*, 88–92. [[CrossRef](#)]
27. Burberry, R.A. Aircraft antennas. *Aeronaut. J.* **1989**, *93*, 58–65. [[CrossRef](#)]
28. Young, J.; Butler, C. Inductance of a shielded coil. *IEEE Trans. Antennas Propag.* **2001**, *49*, 944–953. [[CrossRef](#)]
29. Labun, J.; Fábry, S.; Češkovič, M.; Kurdel, P. Mechanical demodulation of aircraft antenna signal. *Transp. Res. Procedia* **2017**, *28*, 149–155. [[CrossRef](#)]
30. Ferreira, R.C.; Facina, M.S.P.; de Figueiredo, F.A.P.; Fraidenaich, G.; de Lima, E.R. Large Intelligent Surfaces Communicating Through Massive MIMO Rayleigh Fading Channels. *Sensors* **2020**, *20*, 6679. [[CrossRef](#)]
31. Bantan, R.A.R.; Chesneau, C.; Jamal, F.; Elgarhy, M.; Tahir, M.H.; Ali, A.; Zubair, M.; Anam, S. Some New Facts about the Unit-Rayleigh Distribution with Applications. *Mathematics* **2020**, *8*, 1954. [[CrossRef](#)]
32. Antonino-Daviu, E.; Fabres, M.; Ferrando-Bataller, M.; Penarrocha, V.M.R. Modal Analysis and Design of Band-Notched UWB Planar Monopole Antennas. *IEEE Trans. Antennas Propag.* **2010**, *58*, 1457–1467. [[CrossRef](#)]
33. Bhattacharyya, A.; Pal, J.; Patra, K.; Gupta, B. Bandwidth-Enhanced Miniaturized Patch Antenna Operating at Higher Order Dual-Mode Resonance Using Modal Analysis. *IEEE Antennas Wirel. Propag. Lett.* **2020**, *20*, 274–278. [[CrossRef](#)]
34. Jabire, A.H.; Zheng, H.-X.; Abdu, A.; Song, Z. Characteristic Mode Analysis and Design of Wide Band MIMO Antenna Consisting of Metamaterial Unit Cell. *Electronics* **2019**, *8*, 68. [[CrossRef](#)]
35. Wang, Y.; Liu, R.Q.; Yang, H.; Wang, B. Optimization Design and Modal Analysis of Satellite SAR Deployable Support Structure. *Appl. Mech. Mater.* **2014**, *635–637*, 185–189. [[CrossRef](#)]
36. Potgieter, B.R.; Venter, G. Experimental Modal Analysis and Model Validation of Antenna Structures. *Int. J. Mech. Mechatron. Eng.* **2009**, *3*, 1380–1384.
37. García, K.L.; Maes, K.; Parnás, V.E.; Lombaert, G. Operational modal analysis of a self-supporting antenna mast. *J. Wind. Eng. Ind. Aerodyn.* **2020**, *209*, 104490. [[CrossRef](#)]
38. Főző, L.; Andoga, R. Advanced Control of an Electric Fuel-Oil Pump for Small Turbojet Engines. *Aerospace* **2022**, *9*, 607. [[CrossRef](#)]
39. Ward, J. Phase Noise Induced by a Vibrating Antenna. *IEEE Trans. Mic. Theor. Tech.* **2017**, *65*, 4148–4153. [[CrossRef](#)]
40. Zhai, X.; Luo, Y.; Xie, S.; Xu, M.; Zhang, X. Active vibration control of loop antenna structure. *Int. J. Appl. Electromagn. Mech.* **2019**, *59*, 951–958. [[CrossRef](#)]
41. Chen, X.; Tang, Y.; Liu, L.; Zhao, M.; Punyamurtula, V.K.; Chen, J.; Qiao, Y. High-frequency vibration of a conformal antenna structure. *Proc. Inst. Mech. Eng. Part G J. Aerosp. Eng.* **2008**, *222*, 569–574. [[CrossRef](#)]

Disclaimer/Publisher’s Note: The statements, opinions and data contained in all publications are solely those of the individual author(s) and contributor(s) and not of MDPI and/or the editor(s). MDPI and/or the editor(s) disclaim responsibility for any injury to people or property resulting from any ideas, methods, instructions or products referred to in the content.